



ELSEVIER

Journal of Alloys and Compounds 311 (2000) 241–247

Journal of
ALLOYS
AND COMPOUNDS

www.elsevier.com/locate/jallcom

Standard enthalpies of formation of some 5d transition metal gallides by high-temperature direct synthesis calorimetry

S.V. Meschel*, O.J. Kleppa

The University of Chicago, James Franck Institute, 5640 S. Ellis Ave, Chicago, IL 60637, USA

Received 9 June 2000; accepted 29 June 2000

Abstract

The standard enthalpies of formation of some 5d transition metal gallides have been measured by high-temperature direct synthesis calorimetry at 1373 ± 2 K. The following results (in kJ/mol of atoms) are reported: LaGa_2 (-69.2 ± 2.4); HfGa_3 (-42.4 ± 2.7); Hf_5Ga_3 (-45.4 ± 2.1); Ta_5Ga_3 (-28.3 ± 2.2); OsGa_3 (-27.4 ± 1.6); IrGa_3 (-41.2 ± 1.9); IrGa (-43.3 ± 1.8); Pt_3Ga (-41.3 ± 2.2); PtGa (-57.3 ± 2.3). The results are compared with some earlier values obtained by solution calorimetry or derived from EMF measurements. They are also compared with the predicted values of Miedema and coworkers. We compare the enthalpies of formation of 3d, 4d and 5d transition metal gallides and the heats of formation of the 5d gallides with available values for the 5d transition metal aluminides and germanides. © 2000 Elsevier Science S.A. All rights reserved.

Keywords: Transition metal compounds; Heat capacity; Thermodynamic properties; Calorimetry

1. Introduction

During recent years we have, in this laboratory, conducted systematic studies of the thermochemistry of transition metal and rare earth compounds with elements in the IIIB and IVB columns in the periodic table [1]. These investigations have included studies of borides, aluminides, silicides and germanides of the transition metals and the lanthanide elements. The earlier work in this general area by Topor and Kleppa was based on the high-temperature solute–solvent drop technique [2]. In our more recent studies of transition metal silicides, germanides, aluminides and stannides, the direct synthesis method has been used [3–9].

A few years ago we initiated a systematic study of the thermochemical behavior of transition metal gallides. We first demonstrated in our work on PdGa and Pd_2Ga that our values obtained by the direct synthesis method were fully compatible with the results obtained by other methods [10]. Very recently, we also reported on the enthalpies of formation of some 3d and 4d transition metal gallides [11,12]. In the present communication we continue this study and report new data for some 5d transition metal gallides.

We searched the literature for thermochemical information on the 5d gallides and found that very few systems have been studied. However, the gallides of Pt were studied by calorimetry by Vogelbein et al. [13], by Anres et al. [14] and by the EMF method by Katayama et al. [15]. Anres et al. also carried out a detailed calorimetric study of the liquid alloys of Ir–Ga at temperatures between 423 and 763 K [16]. The La–Ga system was studied by the EMF method by Vnuchkova et al. [17].

In the present communication we report new thermochemical data for some phases in the binary systems La–Ga, Hf–Ga, Ta–Ga, Os–Ga, Ir–Ga and Pt–Ga, all obtained by high-temperature direct synthesis calorimetry.

Information regarding some of the phase diagrams and the structures of some of the considered phases is now available in the literature [18]. However, there are no published phase diagrams for the W–Ga, Re–Ga, Os–Ga and Ir–Ga systems and the phase diagram for the Ta–Ga system is incomplete. We also found that the structures of six of the considered compounds were not listed in the ASTM powder diffraction file.

We will compare our results with the reported earlier data for the considered compounds. We will also compare our values with predictions based on the semi-empirical model of Miedema and coworkers [19].

Our thermochemical measurements allow us to obtain a systematic picture of the enthalpies of formation of the 5d

*Corresponding author.

E-mail address: meschel@control.uchicago.edu (S.V. Meschel).

transition metal gallides in their dependence on the atomic number of the transition metal. We can now also compare this dependence for the 3d, 4d and 5d gallides. Finally, we will compare the heats of formation of the 5d transition metal gallides with the corresponding values for the 5d aluminides and germanides. We are now extending this study to the gallides of the lanthanide elements.

2. Experimental and materials

Most of the experiments were carried out at 1373 ± 2 K in a single-unit differential microcalorimeter which has been described in an earlier communication from this laboratory [20]. A few experiments were carried out at 1473 K. All the experiments were performed under a protective atmosphere of argon gas, which was purified by passing it over titanium chips at 900°C . A boron nitride (BN) crucible was used to contain the samples.

The materials were purchased from Johnson Matthey/Aesar, Ward Hill, MA, USA; La and Ga were in ingot form. The purities and particle sizes of the materials are summarized in Table 1. Ga melts at 29°C . We were able to powder Ga by keeping the ingot in the refrigerator and filing it for short periods of time. We described this technique in our previous communications [11,12]. The two components were carefully mixed in the appropriate molar ratio, pressed into 4-mm pellets and dropped into the calorimeter from room temperature.

In a subsequent set of experiments, the reaction products were dropped into the calorimeter to measure their heat contents. Between the two sets of experiments the samples were kept in a vacuum desiccator to prevent reaction with oxygen or moisture.

Calibration of the calorimeter was achieved by dropping weighed segments of high purity, 2-mm Cu wire into the calorimeter at 1373 ± 2 K. The enthalpy of pure Cu at 1373 K, 43.184 kJ/mol of atoms, was obtained from Hultgren et al. [21]. The calibrations were reproducible within $\pm 1.4\%$.

The reacted samples were examined by X-ray diffraction

to assess their structures and to ascertain the absence of unreacted metals. The results of the analyses were conclusive; hence we did not feel the need to check the samples further by X-ray microprobe analysis. All the alloys we studied in this communication were fully reacted except Hf_5Ga_3 . In the other alloys we saw no evidence of unreacted metals within the limits of sensitivity of the diffractometer. For compounds where the X-ray diffraction patterns were not listed in the ASTM powder diffraction file, we generated the patterns from available unit cell parameters and atomic coordinates in Pearson's compilation of crystallographic data [22].

The phase diagram of the La–Ga system shows one congruently melting phase, namely LaGa_2 (m.p. 1450°C) [18]. We prepared this compound in the calorimeter. The X-ray diffraction pattern of LaGa_2 was generated from available unit cell parameters and atomic coordinates [22]. The pattern of our product matched well the generated pattern. There was no evidence of unreacted La or Ga. However, we observed less than 5% of second phase, LaGa .

The phase diagram of the Hf–Ga system shows several intermetallic phases [18]. Hf_5Ga_3 and Hf_5Ga_4 are shown as congruently melting phases, while HfGa , Hf_2Ga_3 , HfGa_2 and HfGa_3 are listed as peritectically melting compounds. The melting points are not given. Hf_5Ga_4 and HfGa have no published structures [22]. We attempted to prepare Hf_5Ga_3 and HfGa_3 in the calorimeter. The X-ray diffraction patterns of these compounds were generated from available unit cell parameters and atomic coordinates [22]. The pattern of Hf_5Ga_3 showed good agreement with the generated pattern; however, we also found a substantial amount of unreacted Hf at 1100°C . We did not observe any other secondary phases. At 1200°C we still noticed about 2–3% unreacted Hf. We attempted to add excess Ga to drive the reaction to completion. We discussed this method in detail in an earlier communication [23]. However, upon addition of 5 mol% and 10 mol% of excess Ga in subsequent samples, the product showed 10–15% of a second phase, most likely Hf_5Ga_4 . We cannot be completely certain about the identity of the second phase since Hf_5Ga_4 has no published structure. However, the lines did not match any other existing Hf–Ga compound. The pattern of HfGa_3 showed excellent agreement with the generated pattern. There was no unreacted Hf or Ga within the limits of sensitivity of the diffractometer. However, we did observe less than 3% of a second phase, HfGa_2 .

The Ta–Ga phase diagram is incomplete [18]. Several intermetallic phases have been predicted, but their melting points are not given. We attempted to prepare Ta_5Ga_3 and TaGa_3 in the calorimeter. The X-ray diffraction pattern of TaGa_3 was generated from the available unit cell parameters and atomic coordinates [22]. The experimental pattern of our TaGa_3 showed a mixed phase. We noticed some TaGa_3 , a substantial amount of Ta_5Ga_3 and also some

Table 1
Purities and particle sizes of the elements used in this study

Element	Metallic purity, %	Particle size
La	99.9	Filed from ingot
Hf	99.6	–325 mesh
Ta	99.98	–325 mesh
W	99.9	12 μ
Re	99.99	–325 mesh
Os	99.8	–200 mesh
Ir	99.95	–60 mesh
Pt	99.9	–200 mesh
Ga	99.999	Filed from ingot

unreacted Ta. Ta_5Ga_3 exists in three structural modifications. Tetragonal, (W_5Si_3 type), tetragonal (Cr_5B_3 type), and hexagonal (Mn_5Si_3 type). The pattern of our reaction product showed that the predominant phase was the tetragonal, W_5Si_3 modification; however, we also found about 5% of the hexagonal modification. We found no unreacted elements or any other secondary phases.

There is no published phase diagram for the W–Ga system [18]. However, the existence of W_2Ga_5 is predicted. We attempted to prepare this compound in the calorimeter, but we found that the product was mostly unreacted.

The hypothetical phase diagram for the Re–Ga system was drawn based on the assumed absence of intermetallic compounds [18]. However, the structures of two modifications of $ReGa_3$ have been reported [22,24]. We attempted to prepare this compound. The X-ray diffraction pattern of our product did not fit the pattern for the l.t. modification of $ReGa_3$ in the ASTM powder diffraction file. Our pattern also showed that while some of the h.t. modification of $ReGa_3$ did form, the reaction was far from complete. We observed more than 50% of unreacted Re and Ga.

There is no phase diagram available for the Os–Ga system [18]. The structure of $OsGa_3$ was determined by Schubert et al. [25] to be a tetragonal, $CoGa_3$ type. Popova and Fomicheva also report having synthesized $OsGa_3$ and $OsGa_2$ at 570–1120 K under pressure [24]. The authors report that $OsGa_3$ is isostructural with $ReGa_3$ (orthorhombic). We prepared $OsGa_3$ in the calorimeter. The X-ray diffraction pattern of the orthorhombic modification is listed in the ASTM powder diffraction file; however, the pattern of the tetragonal modification is not available. We generated this latter pattern from available unit cell parameters and atomic coordinates [22]. Our experimental pattern agreed well with the generated pattern of the tetragonal modification. We found no unreacted elements or any other secondary phases or even the orthorhombic modification.

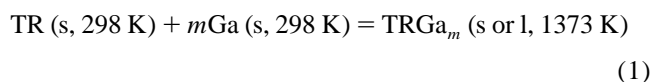
There is no published phase diagram for the Ir–Ga system. However, four intermetallic phases have been reported, namely $IrGa_3$, Ir_2Ga_9 , Ir_3Ga_5 and $IrGa$ [18]. We prepared $IrGa_3$ in the calorimeter at 1100°C and $IrGa$ at 1200°C. Our $IrGa$ product showed no detectable unreacted Ir or any other secondary phases within the limits of the diffractometer. Our pattern for $IrGa_3$ showed excellent agreement with the pattern in the ASTM powder diffraction file. We observed no unreacted components or any secondary phases.

The phase diagram of the Pt–Ga system shows two congruently melting phases, $PtGa$ (m.p. 1104°C) and Pt_3Ga (m.p. 1374°C) [18]. We prepared $PtGa$ at 1200°C and Pt_3Ga at 1100°C in the calorimeter. The phase Pt_3Ga exists in two modifications, with a cubic and a tetragonal structure. The X-ray diffraction patterns of these phases

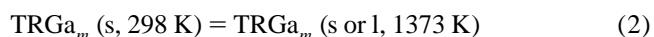
were generated from available unit cell parameters and atomic coordinates [22]. The pattern for our sample of Pt_3Ga agreed well with that of the cubic modification. The X-ray diffraction pattern of $PtGa$ showed excellent agreement with the pattern in the ASTM powder diffraction file; however, we noticed a small amount of Pt_3Ga , about 5%.

3. Discussion

The standard enthalpies of formation of the 5d transition metal gallides determined in this study were obtained as the difference between the results of two sets of measurements. In the first set the following reaction takes place in the calorimeter:



Here m represents the molar ratio Ga/TR, TR represents La, Hf, Ta, Os, Ir, Pt, while s denotes solid and l denotes liquid. The reacted pellets were reused in a subsequent set of measurements to determine their heat contents:



The standard enthalpy of formation is given by:

$$\Delta H_f^0 = \Delta H(1) - \Delta H(2) \quad (3)$$

where $\Delta H(1)$ and $\Delta H(2)$ are the enthalpy changes per mole of atoms in the compound associated with the reactions in Eqs. (1) and (2).

The experimental data are summarized in Table 2. The second column shows the melting points of the phases (where known), while the third column indicates the structure. The heat effects associated with the reactions in Eqs. (1) and (2) are given in kilojoules per mole of atoms as the averages of five–seven consecutive measurements with the appropriate standard deviations. The last column shows the standard enthalpy of formation of the considered phases. The standard deviation given in the last column also reflects the small contributions from the uncertainties in the calibrations. The enthalpies of formation of Hf_5Ga_3 , $IrGa$ and $PtGa$ were measured at 1200°C. We list the value for Hf_5Ga_3 as indicative since we found about 3% unreacted Hf in the sample.

In Table 3 we compare our results with previous experimental values obtained by solution calorimetry [13], by direct synthesis calorimetry [14,16] or derived from EMF measurements [15,17]. The values obtained from the latter studies are at the operating temperature. We list the reference state for Ga in a separate column. Note that there are very few experimental measurements for the 5d gallides. The enthalpy of formation of $IrGa_3$ reported by

Table 2

Summary of the measured standard enthalpies of formation of some 5d transition metal gallides^a

Compound	m.p. ^b °C	Structure	$\Delta H(1)$	$\Delta H(2)$	ΔH_f°
LaGa ₂	1450(c)	AlB ₂	$-40.5 \pm 2.1(6)$	$28.7 \pm 1.1(7)$	-69.2 ± 2.4
HfGa ₃	—	TiAl ₃	$-5.2 \pm 1.5(6)$	$37.2 \pm 2.3(6)$	-42.4 ± 2.7
Hf ₅ Ga ₃ ^c	—	Mn ₅ Si ₃	$-12.9 \pm 1.2(6)^d$	$32.5 \pm 1.7(5)^d$	-45.4 ± 2.1
Ta ₅ Ga ₃	—	W ₅ Si ₃	$2.3 \pm 1.7(7)$	$30.6 \pm 1.4(5)$	-28.3 ± 2.2
OsGa ₃	—	CoGa ₃	$1.8 \pm 1.1(6)$	$29.2 \pm 1.2(5)$	-27.4 ± 1.6
IrGa ₃	—	CoGa ₃	$3.4 \pm 0.9(7)$	$44.6 \pm 1.7(7)$	-41.2 ± 1.9
IrGa	—	CsCl	$-10.1 \pm 1.5(7)^d$	$33.2 \pm 1.0(6)^d$	-43.3 ± 1.8
PtGa	1104(c)	FeSi	$-11.6 \pm 1.6(7)^d$	$45.7 \pm 1.6(7)^d$	-57.3 ± 2.3
Pt ₃ Ga	1374(c)	AuCu ₃	$-8.1 \pm 1.5(6)$	$33.2 \pm 1.6(5)$	-41.3 ± 2.2

^a Data in kJ/mol of atoms. Numbers in parentheses indicate the numbers of experiments averaged. Measurements have been carried out at 1100°C unless otherwise indicated.

^b c = congruently melting compound.

^c Indicative value.

^d Measurements at 1200°C.

Anres et al. obtained by solution calorimetry in liquid Ga (-80 kJ/mol of atoms) has a calculation error [16]. If we make the correct calculation, we get -52 ± 5 kJ/mol of atoms; this is more compatible with our results. Our value for Pt₃Ga agrees well with the value measured by Vogelbein et al. by calorimetry in liquid tin [13]. If we make the appropriate correction for the heat of fusion of Ga (5.6 kJ/mol of atoms cited from Hultgren [21]) the agreement is even better (-42.3 kJ/mol of atoms for Pt₃Ga at 1000 K). Our value for the enthalpy of formation of PtGa agrees well with both the calorimetric value of Anres et al. [14] and with the value derived from EMF data by Katayama et al. [15]. Our result for the heat of formation of LaGa₂ is

not very different from the value derived from the EMF measurements of Vnuchkova et al. [17].

The last column in Table 3 shows the enthalpies of formation predicted on the basis of the semi-empirical model of Miedema and coworkers [19]. Our experimental values agree well with the predicted values for LaGa₂, HfGa₃, Ta₅Ga₃, IrGa and Pt₃Ga. For OsGa₃ and IrGa₃ the experimental heats of formation are considerably more exothermic, while for Hf₅Ga₃ and PtGa the experimental values are less exothermic than the predicted values.

In Fig. 1 the standard enthalpies of formation of 3d, 4d and 5d transition metal gallides are plotted against the atomic number of the transition metal. The molar com-

Table 3

Comparison of the standard enthalpies of formation with some experimental data in the literature and with predicted values from the semi-empirical model of Miedema and coworkers [19]^a

Compound	ΔH_f° (Experimental) This work	ΔH_f° (Experimental) Literature	Ref. State Ga	Method Ref.	ΔH_f° (Predicted)
LaGa ₂	-69.2 ± 2.4	-74.6	1	EMF (17) ΔG_f , 975 K	-68
HfGa ₃	-42.4 ± 2.7	—	—	—	-44
Hf ₅ Ga ₃ ^b	-45.4 ± 2.1	—	—	—	-61
Ta ₅ Ga ₃	-28.3 ± 2.2	—	—	—	-29
OsGa ₃	-27.4 ± 1.6	—	—	—	-17
IrGa ₃	-41.2 ± 1.9	$-80(-52 \pm 5)$	s	Soln. Calor. (Ga), 1482 K (16)	-29
IrGa	-43.3 ± 1.8	—	—	—	-47
PtGa	-57.3 ± 2.3	-56.4	s	Soln. Calor. (Ga), 1350 K (14)	-73
		-56.3	1	EMF (15) ΔG_f , 1100 K	
Pt ₃ Ga	-41.3 ± 2.2	-43.7	1	Soln. Calor. (Sn), 1000 K (13)	-46

^a Data in kJ/mol of atoms.

^b Indicative value.

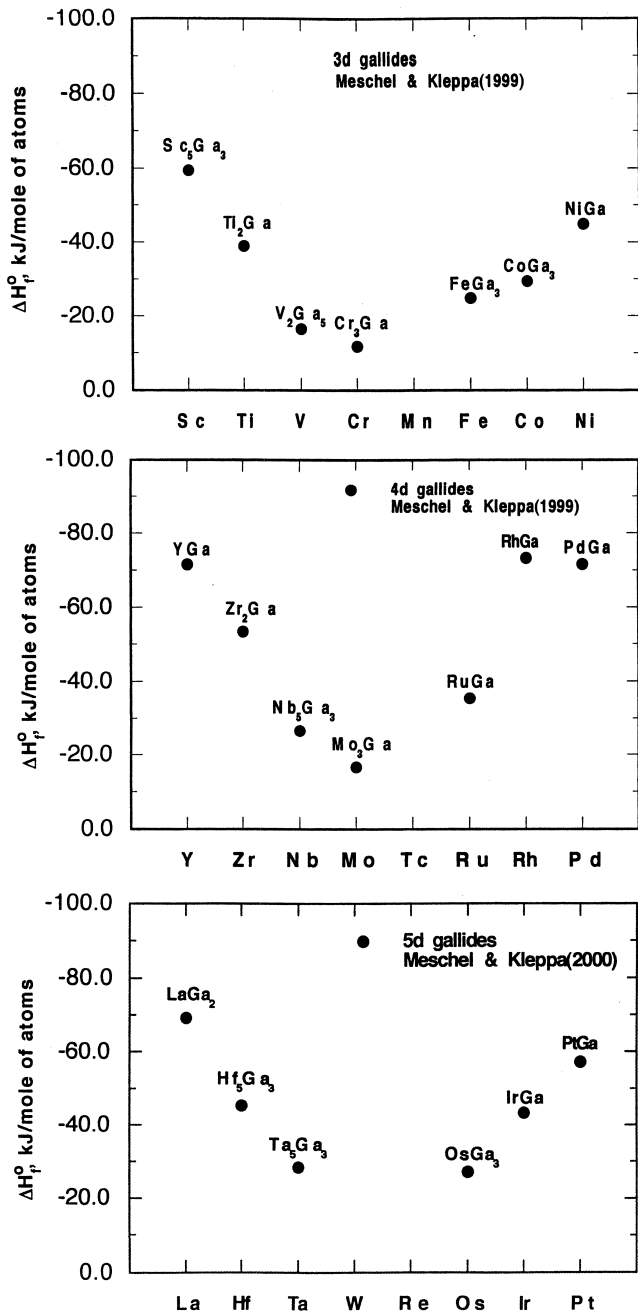


Fig. 1. Standard enthalpies of formation of some 3d, 4d and 5d transition metal gallides. Data in kJ/mol of atoms.

positions of the alloys are indicated in the figure. In this figure we always plotted our most exothermic enthalpy of formation for each binary system. Note that we have no quantitative values for *W* and *Re*. However, on the basis of our observations of the heat effects in the partially formed ReGa_3 we infer that the magnitude of the enthalpy of formation is in the range between -10 and 20 kJ/mol of atoms. The figure shows that the enthalpies of formation of

the 5d gallides decline in magnitude from La to Ta and subsequently the values increase from Os to Pt. The shapes of the three curves are very similar; they are roughly parabolic with the minima in approximately the same location. This is consistent with the prediction by Pasturel et al. for transition metal aluminides [26]. It is also noteworthy that the 4d alloys have the highest exothermic enthalpies of formation among the 3d, 4d and 5d gallides. We observed similar behavior for the transition metal aluminides, silicides, germanides and stannides previously studied in this laboratory [27].

In Fig. 2 we compare our enthalpies of formation for the 5d gallides with values for the 5d aluminides determined by Jung and Kleppa [4,5] and by Meschel and Kleppa [6]. This figure shows that qualitatively the shapes of the curves are similar; both are roughly parabolic, and the minima are in the same location. From La to Ta the values are very similar; from Os to Pt the values for the aluminides are considerably more exothermic than for the gallides.

In Fig. 3 we compare our enthalpies of formation for the 5d gallides with values for the 5d germanides determined by Jung and Kleppa [8,9] and by Meschel and Kleppa [6]. This figure shows that while for La the values are practically the same, for Hf and Ta the germanides are more exothermic, while from Os to Pt the gallides are more exothermic than the germanides.

In our study of the 3d and 4d transition metal gallides and also of the 3d, 4d and 5d aluminides we found no correlation between the observed enthalpies of formation and the difference in the electronegativities of the two components of the alloy [27]. The same situation holds for the 5d gallides. For example, the electronegativity difference between transition metal and gallium is the same for Os, Ir and Pt, while the enthalpies of formation of Os and Ir gallides differ by approximately a factor of two (these alloys have the same stoichiometry). This suggests that the chemical bonding for the transition metal gallides are covalent rather than ionic as was noted for aluminides by Colinet et al. [28]. We cannot make a comparison of the melting points with the enthalpies of formation. Such data are not available for most of the alloys which we studied. In our previous communications we found no correlation between the melting points and the heats of formation for the 3d and 4d gallides and for the aluminides [6,11,12].

We noted in earlier work that the enthalpies of formation of alloys of the lanthanide elements with the IIIB elements in the periodic table show a roughly parabolic correlation when plotted against the IIIB elements [27,29]. We also found this correlation for the Sc and Y compounds [29]. Where data are available, the enthalpies of formation of the gallides seem to have the most exothermic values among the IIIB compounds. In Fig. 4 we show an example of this trend for the La alloys. The enthalpies of formation of LaIn_3 , and LaTl_3 were measured by Palenzona and Cirafici

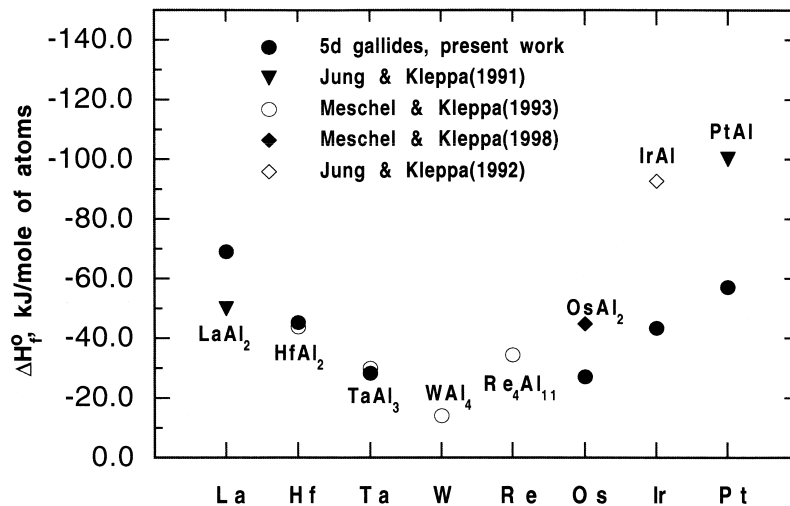


Fig. 2. Comparison of the enthalpies of formation of some 5d transition metal gallides and aluminides. Data in kJ/mol of atoms. The stoichiometric composition of the 5d gallides is shown on Fig. 1.

[30]. The enthalpies of formation of the transition metal alloys show a somewhat different picture. In our study of the 5d silicides we found that in the family of IVB compounds, the silicides usually have the highest negative enthalpies of formation [6]. For compounds of IIIB elements the correlation is not as clear. For many of the transition metal binaries the alloys with In and Tl either do not form or the heats of formation are not available for comparison. The aluminides in some cases have more negative enthalpies of formation than the gallides. We find that for Fe, Co, Ni, Mo, Ru, Rh, Pd, Os, Ir, Pt the aluminides have the numerically highest values. However,

for Sc, Ti, Cr, Zr, Nb, Hf, Ta the borides have the most exothermic enthalpies of formation.

Acknowledgements

This investigation has been supported by the Department of Energy under Grant DE-FG02-88ER4563, and has benefited from the MRSEC facilities at the University of Chicago. We are indebted to Dr Joseph Pluth for his help with generating the X-ray diffraction patterns from the reported unit cell parameters and atomic coordinates.

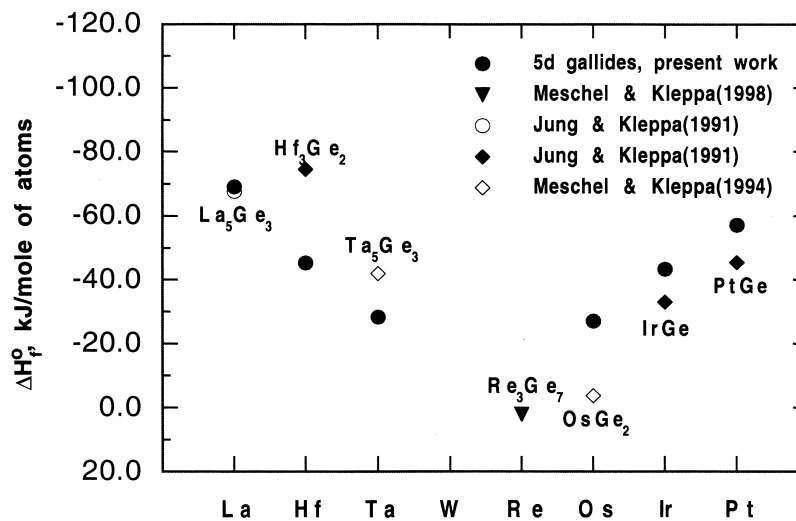


Fig. 3. Comparison of the enthalpies of formation of 5d transition metal gallides and germanides. Data in kJ/mol of atoms. The stoichiometric composition of the 5d gallides is shown on Fig. 1.

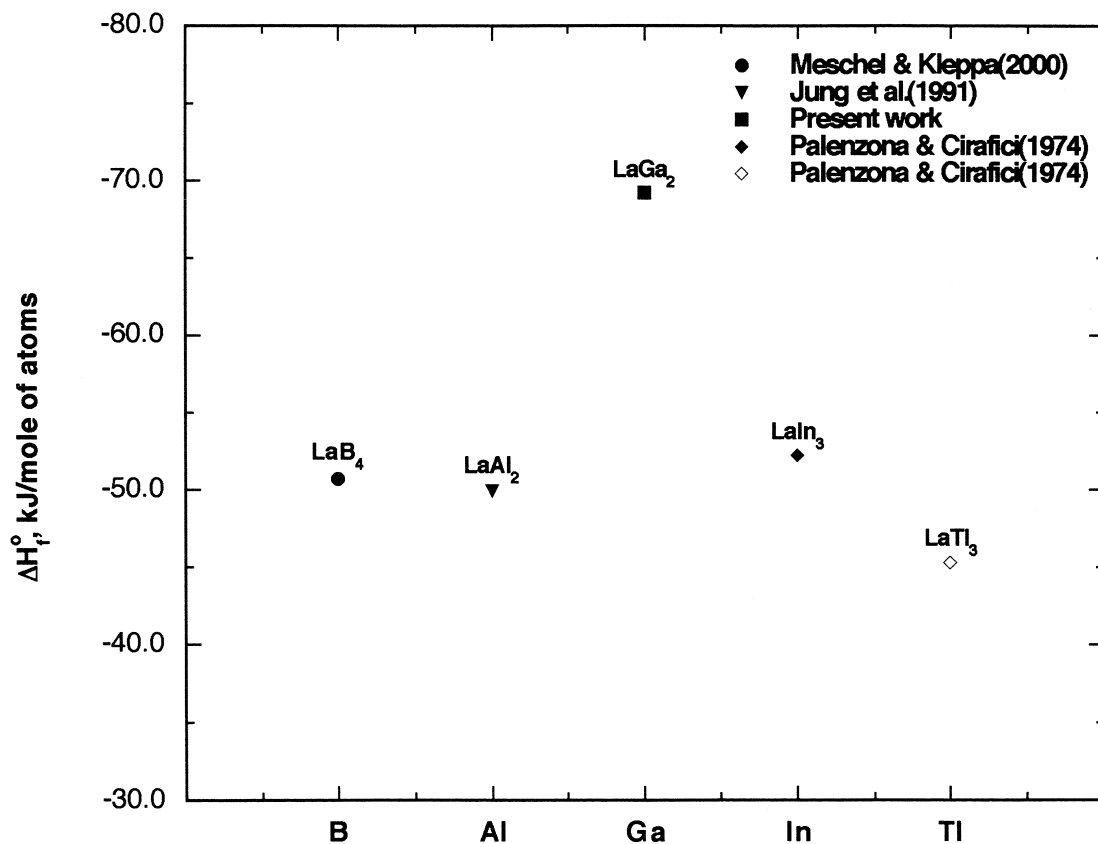


Fig. 4. Comparison of the enthalpies of formation of alloys of La with IIIA elements in the periodic table. Data in kJ/mol of atoms.

References

- [1] O.J. Kleppa, *J. Phase Equil.* 15 (1994) 240–263.
- [2] L. Topor, O.J. Kleppa, *J. Chem. Thermodyn.* 16 (1984) 993–1002.
- [3] S.V. Meschel, O.J. Kleppa, *J. Alloys Comp.* 197 (1993) 75–81.
- [4] W.G. Jung, O.J. Kleppa, L. Topor, *J. Alloys Comp.* 176 (1991) 309–318.
- [5] G.W. Jung, O.J. Kleppa, *Metall. Trans.* 23B (1992) 53–56.
- [6] S.V. Meschel, O.J. Kleppa, *J. Alloys Comp.* 280 (1998) 231–239.
- [7] S.V. Meschel, O.J. Kleppa, *Thermochim. Acta* 314 (1998) 205–212.
- [8] W.G. Jung, O.J. Kleppa, *J. Alloys Comp.* 176 (1991) 301–308.
- [9] W.G. Jung, O.J. Kleppa, *J. Alloys Comp.* 169 (1991) 85–92.
- [10] S.V. Meschel, O.J. Kleppa, *Thermochim. Acta* 292 (1997) 13–17.
- [11] S.V. Meschel, O.J. Kleppa, *J. Alloys Comp.* 290 (1999) 150–156.
- [12] S.V. Meschel, O.J. Kleppa, *J. Alloys Comp.* 297 (2000) 162–167.
- [13] W. Vogelbein, M. Ellner, B. Predel, *Thermochim. Acta* 44 (1981) 141–149.
- [14] P. Anres, M. Gaune-Escard, J.P. Bros, *J. Alloys Comp.* 234 (1996) 264–274.
- [15] I. Katayama, T. Makino, T. Iida, *High Temp. Mater. Sci.* 34 (1995) 127–135.
- [16] P. Anres, M. Gaune Escard, J.P. Bros, *J. Alloys Comp.* 259 (1997) 225–233.
- [17] L.A. Vnuchkova, A.P. Bayanov, V.V. Serebrennikov, *Russ. J. Phys. Chem.* 45 (1971) 99.
- [18] T.B. Massalski, H. Okamoto, P.R. Subramanian, L. Kacprzak (Eds.), *Binary Alloy Phase Diagrams*, second ed, ASM, Metals Park, OH, 1990.
- [19] F.R. de Boer, R. Boom, W.C.M. Mattens, A.R. Miedema, A.K. Niessen, *Cohesion in Metals, Transition Metal Alloys*, North Holland, Amsterdam, 1988.
- [20] L. Topor, O.J. Kleppa, *Thermochim. Acta* 139 (1989) 291–297.
- [21] R. Hultgren, P.D. Desai, D.T. Hawkins, M. Gleiser, K.K. Kelley, D.D. Wagman (Eds.), in: *Selected Values of the Thermodynamic Properties of the Elements*, ASM, Metals Park, OH, 1973, p. 154.
- [22] P. Villars, L.D. Calvert (Eds.), *Pearson's Handbook of Crystallographic Data for Intermetallic Phases*, ASM, Metals Park, OH, 1985.
- [23] S.V. Meschel, O.J. Kleppa, *J. Chim. Phys.* 90 (1993) 349–354.
- [24] S.V. Popova, L.N. Fomicheva, *Izvest. Akad. Nauk SSSR, Neorg. Mater.* 18 (1982) 251–255.
- [25] K. Schubert, H.L. Lukas, H.G. Meissner, S. Bhan, *Z. Metallkunde* 50 (1959) 534–540.
- [26] A. Pasturel, D. Nguyen Manh, D. Mayou, *J. Phys. Chem. Solids* 47 (1986) 325–330.
- [27] S.V. Meschel, O.J. Kleppa, *J. Alloys Comp.* (2000) submitted.
- [28] C. Colinet, A. Bessoud, A. Pasturel, *Z. Metallkunde* 77 (1986) 798–804.
- [29] S.V. Meschel, O.J. Kleppa, *J. Alloys Comp.* 238 (1996) 180–186.
- [30] A. Palenzona, S. Cirafici, *Thermochim. Acta* 9 (1974) 419–425.